Micromechanical study of the elastic stiffness in frictional granular soils

K. Taghizadeh, V. Magnanimo & S. Luding

MultiScale Mechanics, CTW, MESA+, University of Twente, Enschede, Netherlands

E-mail: `k.taghizadehbajgirani@utwente.nl`

Abstract. Understanding the pre-failure, elastic behavior of dense granular systems is of interest in many fields, such as soil mechanics, material science and physics. The main difficulty is the discreteness and disorder in granular materials at the microscopic scale, which requires a multi-scale approach. The Discrete Element Method (DEM) allows to inspect the influence of microscopic contact properties of its individual constituents on the bulk behavior of granular assemblies. In this study, isotropic deformations are applied to polydisperse packings of both frictionless and frictional spheres; after preparation by isotropic compression of samples with different contact friction, at various volume fractions, the effective bulk modulus is determined from the incremental stress response to the application of strain-probes. As we are interested first in the reversible, elastic response, the amplitude of the applied perturbations has to be small enough to avoid much opening and closing of contacts, which would lead to irreversible rearrangements in the sample. Counterintuitively, with increasing inter-particle contact friction, the bulk modulus decreases for samples with the same volume fraction. We explain this by differences in the microstructure (isotropic fabric) that characterize the samples state after preparation.

1. INTRODUCTION

Granular materials behave differently from usual solids or fluids and show peculiar mechanical properties like dilatancy, history dependence, ratcheting and anisotropy [**?**]. The behavior of these materials is highly non-linear and involves irreversibility (plasticity), possibly already at very small strains, due to rearrangements of the elementary particles [1, 3, 6, 10]. Many industrial and geotechnical applications that are crucial for our society involve granular systems at small strain levels. That is the case of structures designed to be far from failure (e.g. shallow foundations or underlying infrastructure), strains in the soil are small and a sound knowledge of the bulk stiffness is essential for the realistic prediction of ground movements [13]. Finite-element analyses of tunnels depend on the model adopted for the pre-failure soil behaviour. When the surface settlement is considered, the importance of modelling non-linear elasticity and the shear modulus characterization become of outmost importance [**?**]. Design and licensing of critical infrastructure such as nuclear plants and long span bridges is dependent on a robust knowledge of elastic properties in order to calculate seismic ground motion site response characteristics and to confirm geotechnical foundation conditions such as the risk of liquefaction and the presence of anisotropic strata. Critically needed parameters include the seismic shear wave velocity profile and shear moduli/damping characteristics of soil and rock.

When looking at natural flows, a complete description of the granular rheology should include an elastic regime [16]. The onset of failure deserves particular attention in this context. Although

the definition of the elastic parameters have little influence on the predicted factor of safety in classical slope stability analysis (e.g. Method of slices [19]), they have a profound influence on the computed deformations prior to failure [17]. Information on the initial stiffness are usually embedded into the value of the macroscopic friction angle, as obtained e.g. from shear box experiments. However any predictive model must also describe the pre-failure deformation behaviour of the soil. A large amount of study has been devoted on the pre-failure deformation characteristics of geomaterials [20] Recent studies are aimed to relate commonly used intact rock parameters of pre-failure (tangent moduli, secant moduli, peak strength) to the post-failure state [18].

Finally, sediments are one example of particles of organic or inorganic origin that accumulate in a loose, unconsolidated form before they are compacted and solidified; they can be classified as a type of granular materials. Sediments are commonly found in the nature and the knowledge of their mechanical behavior is important in industrial, geotechnical and geophysical applications. For instance, the elastic properties of high-porosity ocean-bottom sediments have a massive impact on unconventional resource exploration and exploitation by ocean drilling programs.

As first-step for a comprehensive modeling of the pre-failure, behavior of the granular soil, we study the simplest case of isotropic material and we focus on the bulk modulus. Recent works [2, 9, 7] show that along with the macroscopic properties (stress and volume fraction) also the structure, quantified by the fabric tensor [5, 6] plays a crucial role, as it characterizes, on average, the geometric arrangement of contacts, i.e. the microstructure of the particle packing.

In this study we use Discrete Element simulations to reproduce granular isotropic samples and study the material behavior as resulting from the sample micro- and macro-characteristics. In order to investigate the elastic response, we perform so-called strain probing tests along an isotropic deformation (pre-strain) path [9, 6]. In the case of a finite assembly of particles, in simulations, a finite elastic regime can always be detected and the elastic stiffnesses can thus be measured by means of an applied very small strain perturbation. We scan a wide range of inter-particle friction coefficients and volume fractions, in order to understand how the interplay of contact and system properties affects the microstructure and thus the elastic moduli.

2. NUMERICAL SIMULATION

The Discrete Element Method (DEM) [6, 8] can help to understand the response to deformation of particle systems. At the basis of DEM are force laws that relate the interaction force to the overlap and tangential displacement of two particle contact surfaces. If all forces $\mathbf{f}_i$ acting on particle i are known, the problem is reduced to the integration of Newton's equations of motion for the translational and rotational degrees of freedom.

2.1. Contact model

For the sake of simplicity, the linear visco-elastic contact model for the normal component of force is used. The simplest normal contact force model is given by $f^n = k\delta + \gamma\dot{\delta}$, where k is the spring stiffness, γ is the contact viscosity parameter, $\delta = (d_i + d_j)/2 - (\mathbf{r}_i - \mathbf{r}_j).\hat{\mathbf{n}}$ is the overlap between two interacting particles i and j, with diameters d_i and d_j, with contact normal vector $\hat{\mathbf{n}} = (\mathbf{r}_i - \mathbf{r}_j)/|(\mathbf{r}_i - \mathbf{r}_j)|$, and $\dot{\delta}$ is the relative velocity in the normal direction. In order to reduce dynamical effects and shorten relaxation times, an artificial viscous background dissipation force $\mathbf{f}_b = -\gamma_b\mathbf{v}_i$ proportional to the moving velocity $\mathbf{v}_i$ of particle i is added, resembling the damping due to a background medium, as e.g. a fluid. The tangential force model introduced in Ref. [8] is used and thus will not be detailed here.

The standard simulation parameters are $N = 4096(= 16^3)$ particles with average radius $\langle r \rangle = 1$ [mm], density $\rho = 2000$ [kg/m^3], elastic stiffness $k = 10^8$ [kg/s^2], particle damping coefficient $\gamma = 1$ [kg/s], and background dissipation $\gamma_b = 0.1$ [kg/s]. This corresponds to a contact duration $t_c = 0.64$ [μs] and coefficient of restitution $e = 0.92$ for two typical particles. The tangential stiffness and viscosity are set as $k_t/k = 0.2$ and $\gamma_t/\gamma_n = 0.2$, while the coefficient

of friction μ is varied. Note that the polydispersity of the system is quantified by the width ($w = r_{\max}/r_{\min} = 3$) of a uniform size distribution, where $r_{\max}$ and $r_{\min}$ are the radii of the biggest and smallest particles respectively. For details about other time scales present in the system, see [4, 6].

2.2. Macroscopic (tensorial) quantities

Here, we define averaged tensorial macroscopic quantities – including strain-, stress- and fabric (structure) tensors – that provide information about the state of the packing and reveal the interesting bulk features.

By speaking about the strain tensor $\mathbf{E}$, we refer to the external (global) strain that we apply to the sample. The isotropic part of the infinitesimal strain, ε_{v}, is defined as: $\varepsilon_{\mathrm{v}} = \dot{\varepsilon}_{\mathrm{v}}\mathrm{d}t = -\left(\varepsilon_{xx} + \varepsilon_{yy} + \varepsilon_{zz}\right)/3 = \mathrm{tr}(-\mathbf{E})/3 = \mathrm{tr}(-\dot{\mathbf{E}}\mathrm{d}t)/3$, where $\varepsilon_{\alpha\alpha} = \dot{\varepsilon}_{\alpha\alpha}\mathrm{d}t$ with $\alpha\alpha = xx$, yy and zz as the diagonal components of the tensor in the Cartesian $x - y - z$ reference system where $\dot{\varepsilon}_{\mathrm{v}}$ is the strain-rate applied during a time-step dt. The trace integral of $3\varepsilon_{\mathrm{v}}$ is denoted as ε_{vol}, the true or logarithmic volumetric strain, i.e., the volume change of the system, relative to the initial reference volume, V_0.

On the other hand, from DEM simulations, one can measure the 'static' stress in the system

$$\boldsymbol{\sigma} = (1/V) \sum_{c \in V} \mathbf{l}^c \otimes \mathbf{f}^c, \tag{1}$$

averaged over all contacts in the volume V, with the dyadic product between the contact force $\mathbf{f}^c$ and the branch vector $\mathbf{l}^c$, where the contribution of the kinetic fluctuation energy has been neglected [4, 5]. The isotropic component of the stress is the pressure $P = \mathrm{tr}(\boldsymbol{\sigma})/3$.

In order to characterize the geometry/structure of the static aggregate at microscopic level, we measure the fabric tensor

$$\mathbf{F} = \frac{1}{V} \sum_{\mathcal{P} \in V} V^{\mathcal{P}} \sum_{c \in \mathcal{P}} \mathbf{n}^c \otimes \mathbf{n}^c \ , \tag{2}$$

weighted according to $V^{\mathcal{P}}$, the particle volume of particle $\mathcal{P}$, for all particles inside the averaging volume V, the normal unit branch-vector $\mathbf{n}^c$ pointing from center of particle $\mathcal{P}$ to contact c [6]. The isotropic fabric is proportional to the volume fraction ν and the coordination number C.

$$F_v = \mathrm{tr}(\mathbf{F}) = g_3 \nu C \ , \tag{3}$$

with a function g_3 of moments of the size distribution and $g_3 \approx 1.22$ for polydispersity $w = 3$. Note that in this work we use $k^* = k/(2\langle r \rangle)$ to non-dimensionalize the stress, i.e. $\boldsymbol{\sigma}^* = \boldsymbol{\sigma}/k^*$.

2.3. Sample preparation and test procedure

In this subsection, we first describe the preparation procedure and then the details of the numerical isotropic test. The preparation procedure is an essential step in any physical/numerical experiment to obtain reproducible and reliable results, especially when friction is involved. The initial configurations is such that spherical particles are randomly generated, with low volume fraction and rather large random velocities in a periodic 3D box, such that they have sufficient space and time to exchange places and to randomize themselves. The initial configurations are obtained by first homogeneously compressing a granular gas up to a volume fraction below the jamming fraction. The system is then relaxed to allow the particles to dissipate kinetic energy and achieve a zero-pressure static configuration [4, 6, 15]. This is followed by an isotropic compression-decompression cycle up to a desired maximum volume fraction $\nu_{\max} = 0.82$, as depicted into Fig.1.a [4, 6, 15], using different coefficients of friction (varying from $\mu = 0$ to 10). Note that this preparation is carried out with strain-control, where at every time-step the particles are moved according to the momentary strain-rate tensor (isotropic, with $\dot{\varepsilon}_{vol} = 38.0 \ [\mu\mathrm{s}^{-1}]$). In Fig.1.b, we show the evolution of the volumetric fabric

F_v with volume fraction ν during decompression for different coefficients of friction ($\mu = 0, 0.1$ and 1). The isotropic fabric at ν_{max} decreases systematically with the coefficient of friction and decreases with decreasing volume fraction ν, due to the decrease of the coordination number, before it suddenly drops to zero at the jamming point.
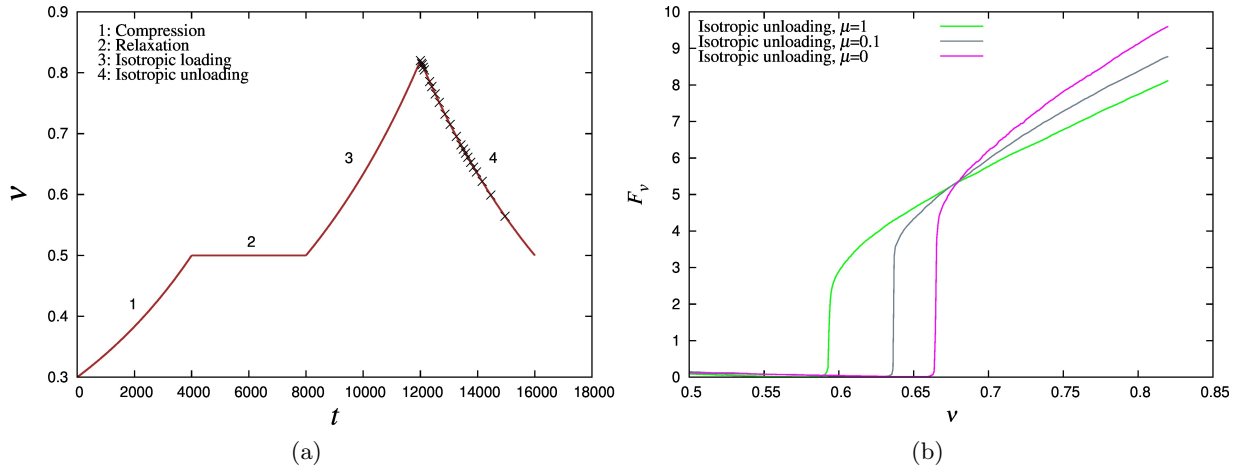

Figure 1. (a) Evolution of volume fraction as a function of time during sample preparation: (1) A frictional granular gas is homogeneously compressed from $\nu = 0.3$ to $\nu = 0.5$; and (2) relaxed at $\nu = 0.5$; (3) the sample is compressed from $\nu = 0.5$ to $\nu = 0.82$; (4) finally, the sample is decompressed from $\nu = 0.82$ to $\nu = 0.5$. Black crosses '$\times$' represent the chosen configurations for further tests. (b) Evolution of isotropic fabric F_v with volume fraction along preparation path for packings with different coefficients of friction ($\mu = 0, 0.1, 1$).

3. BULK MODULUS

We now study the incremental response as function of the contact-friction during isotropic compression.

Various configurations are chosen at different volume fractions above jamming, along the unloading branch, from preparations with different friction. Sufficient relaxation is applied to allow the particles to achieve a static configuration in mechanical equilibrium, before we probe these relaxed samples by applying small strain perturbations thus measuring the incremental stress responses [4, 5, 6, 9]. For each friction we apply an identical strain-rate value $\dot{\varepsilon}_{vol} = 10.0$ [μs^{-1}]. After probing the configurations, the effective bulk modulus of the granular assembly is obtained as the ratio between the measured increment in pressure and the applied isotropic strain:

$$B = \delta P^*/3\delta\varepsilon_{vol} \qquad (4)$$

where P^* is the non-dimensional pressure, $P^* = P/k^*$.

3.1. Evolution of the bulk modulus

As we are interested in the elastic response, we first have to identify the elastic regime, the marginal regime and the plastic regime [6]. For the modulus results presented below, the applied infinitesimal strain step is kept small enough to avoid strong, irreversible particle rearrangements; plasticity (irreversibility) develops in the sample as soon as those rearrangements happen. The bulk modulus and the isotropic fabric for different amplitudes of the applied isotropic strain, $\delta\varepsilon_{vol}$, are depicted for chosen configurations ($\nu = 0.82$, $\mu = 0.0001$ and $\mu = 1$) during probing in

Fig.2. B stays practically constant for small amplitudes ($\delta\varepsilon_{vol} < 10^{-4}$) and the regime can be considered to be elastic [12]. By increasing the amplitudes of the perturbation, $\delta\varepsilon_{vol}$, B starts to increase non-linearly. Comparing Fig.2.a and 2.b, shows that the non-linearity of B is associated with the change in volumetric fabric. The insets in Fig.2.a and 2.b show that for B and ΔF_v, the elastic regime is wider when the friction coefficient is larger, partly due to larger distance from jamming [4].
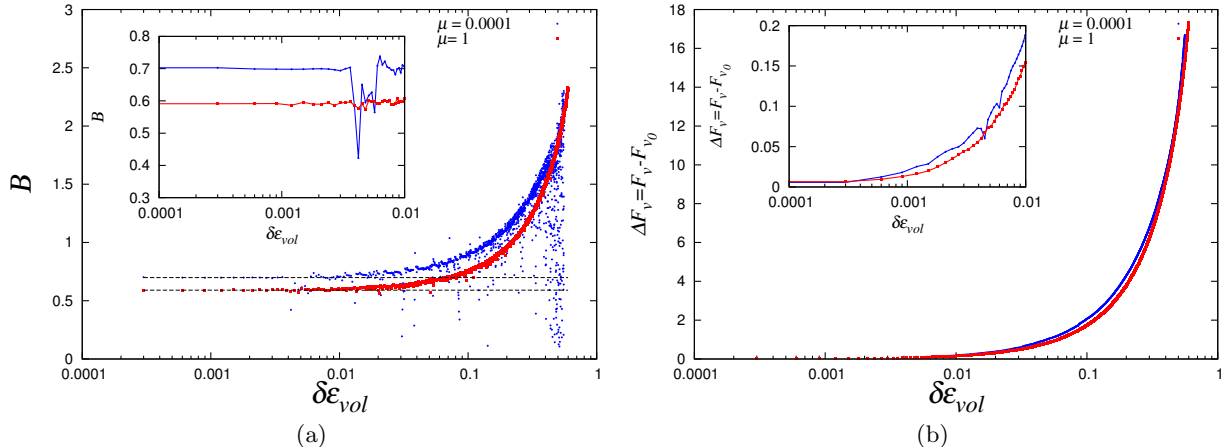

Figure 2. Evolution of (a) bulk modulus B and (b) change in isotropic fabric ΔF_v with volume fraction ν for a configuration at $\nu = 0.82$ and coefficient of friction, $\mu = 0.0001$ and 1, respectively. Note that the x-axis in on log-scale, with inset plots in linear scale.

3.2. Effect of inter-particle contact friction on the bulk modulus

In Fig.3.a, we plot the variation of the bulk modulus B, with volume fraction for packings with different coefficients of friction μ. The bulk modulus always increases with increasing density. However, the increase of the bulk modulus is slower for packings with high friction. We can relate this behavior to a higher average number of contacts (i.e. higher F_v) for samples prepared with low friction (Fig.3.b) at the same volume fraction. The value of the initial fabric is proportional to the number of contacts, and influences the subsequent evolution of the stiffness properties [12].

When the bulk modulus is plotted not against volume fraction, but against the isotropic fabric F_v in Fig.3.b, the data for large $\mu \geq 0.05$ approximately collapse on an unique curve, implying a general relation between bulk stiffness and isotropic micro-structure. The coefficient of friction has no direct influence on the bulk modulus as sliding is not activated in the elastic regime for isotropic pre-strain, but rather it effects B indirectly through the preparation that leads to a different state variable F_v.

Note that frictionless and frictional curves show qualitatively different behavior, associated with the activation of stronger and stronger tangential forces. In general, one can observe three regimes, frictionless, low ($0 < \mu < 0.001$) and higher friction ($0.001 \leq \mu$). The low friction packings behave in a similar fashion to the frictionless ones in the loose regime (close to the jamming volume fraction), but follow the behavior of systems with stronger friction when they are far from the jamming point.

4. CONCLUSIONS

In a triaxial box, the bulk modulus is measured, which describes the incremental, elastic pressure-response of relaxed granular materials to applied small strain perturbations. The tested states
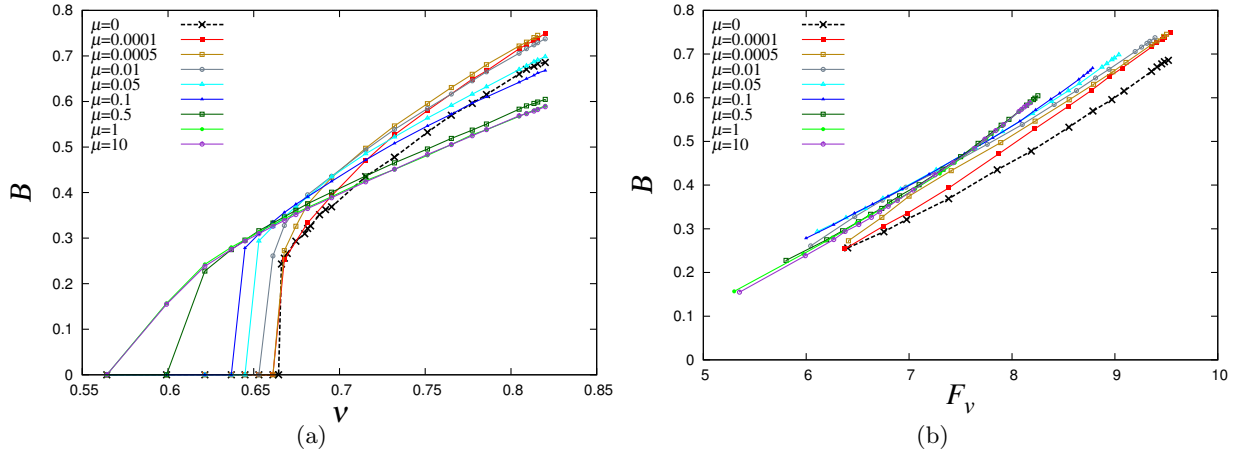
Figure 3. (a) Evolution of the bulk modulus B with volume fraction ν for different coefficients of friction, μ, as shown in the legend. (b) Evolution of the bulk modulus B versus isotropic fabric F_v for various volume fractions and different μ, as shown in the legend.

have experienced different deformation history, since the particles have different properties already during preparation of the tests, like the coefficient of inter-particle contact friction. In this paper, we have focused on the effect of friction on the macroscopic bulk modulus over a wide range of volume fractions.

A relation between the bulk modulus and the isotropic fabric is established in agreement with [6, 14]. Surprisingly, this relation for frictional packings does not follow the same trend as for frictionless packings. The tangential force plays a crucial role in establishing the contact network and thus is very important for the mechanical properties of granular materials. Since frictionless particles are an unrealistic limit-case material, this is a big step towards realistic materials. The tangential force has to be taken into account, even though it carries relatively small magnitudes of force, in the case of low coefficients of friction.

Extension of the work to investigate the influence of inter-particle contact friction on the shear modulus and structural anisotropy is in progress, using the same probing approach. Additional work will focus on establishing a micro-mechanical based constitutive model, involving the elastic regime, with goal to predict the pre-failure behavior of geomaterials.

5. ACKNOWLEDGEMENTS

References

[1] J. P. Bardet (1994). Numerical simulations of the incremental responses of idealized granular materials. *Int. J. of Plasticity*, 10(8), 879-904.

[2] A. Ezaoui and H. Di Benedetto (2009). Experimental measurements of the global anisotropic elastic behaviour of dry Hostun sand during triaxial tests, and effect of sample preparation. *Geotechnique*, 59(7), 621-635.

[3] J. D. Goddard (1990). Nonlinear Elasticity and Pressure-Dependent Wave Speeds in Granular Media. *Proc. R. Soc. Lond. A*, 430(1878), 105-131.

[4] O. I. Imole, N. Kumar, V. Magnanimo, and S. Luding (2013). Hydrostatic and Shear Behavior of Frictionless Granular Assemblies Under Different Deformation Conditions. *KONA*, 30, 84-108.

[5] O. I. Imole, V. Magnanimo, and S. Luding (2014). Micro-Macro Correlations and Anisotropy in Granular Assemblies under Uniaxial Loading and Unloading, Phys. Rev. E 89, 042210.

[6] N. Kumar, S. Luding & V. Magnanimo (2014). Macroscopic model with anisotropy based on micro-macro informations. *Acta Mechanica*, 225(8), 2319-2343.

[7] L. La Ragione and V. Magnanimo (2012). Contact anisotropy and coordination number for a granular assembly: A comparison of distinct-element-method simulations and theory. *Phys. Rev. E.*, 85(3).

[8] S. Luding (2008). Cohesive frictional powders: Contact models for tension Granular Matter 10(4), 235-246.

[9] V. Magnanimo, L. La Ragione, J.T Jenkins, P. Wang & H.A. Makse (2008). Characterizing the shear and bulk moduli of an idealized granular material. *Europhys. Lett.*, 81, 34006.

[10] L. Sibille, F. Nicot, F.-V. Donzoe, and F. Darve (2009). Analysis of failure occurrence from direct simulations. *Eur. J. Env. Civ. Eng.*, 13(2), 187-201.

[11] C. Thornton and L. Zhang (2010). On the evolution of stress and microstructure during general 3D deviatoric straining of granular media. *Géotechnique*, 60(5), 333-341.

[12] V. Magnanimo and L. La Ragione. A micromechanical numerical analysis for a triaxial compression of granular materials. Powders and Grains 2013, American Institute of Physics, 2013, *AIP Conference Proceedings,* vol. 1542, no. 1, pp. 1234-1237.

[13] C. R. I. Clayton (2011). Stiffness at small strain: research and practice. *Gotechnique,* 61(1), 5-37.

[14] F. Göncü, O. Durán and S. Luding (2010). Constitutive relations for the isotropic deformation of frictionless packings of polydisperse spheres. *Comptes Rendus Mécanique*, 338(10), 570-586.

[15] F. Göncü and S. Luding (2013). Effect of particle friction and polydispersity on the macroscopic stress-strain relations of granular materials. *Acta geotechnica*, 8.6 (2013): 629-643.

[16] C.S.Campbell (2006). Granular material flowsan overview. *Powder Technology*, 162.3 (2006): 208-229.

[17] D.V. Griffiths and P.A. Lane (1999). Slope stability analysis by finite elements. *Geotechnique*, 49.3 (1999): 387-403.

[18] L. Tutluolu, l.F. Oğe and C. Karpuz (2015). Relationship between pre-failure and post-failure mechanical properties of rock material of different origin. *Rock Mechanics and Rock Engineering*, 48.1 (2015): 121-141.

[19] A.W. Bishop (1955). The use of the slip circle in the stability analysis of slopes. *Geotechnique*, 5 (1955): 7-17.

[20] M.B. Jamiolkowski, R. Lancellotta, D.L. Presti (1999). Pre-failure Deformation Characteristics of Geomaterials.

[21] T.L Addenbrooke, D.M. Potts and A.M Purzin (1998). The influence of pre-failure soil stiffness on the numerical analysis of tunnel construction. *Pre-failure Deformation Behaviour of Geomaterials*, 307.

[22] T.L Addenbrooke, D.M. Potts and A.M Purzin (1998). The influence of pre-failure soil stiffness on the numerical analysis of tunnel construction. *Pre-failure Deformation Behaviour of Geomaterials*, 307.